

Update on pion scalar radii with $N_f = 2+1$ Clover-improved Wilson fermions

Konstantin Ottnad^a, Georg von Hippel^a

^a Institut für Kernphysik, Johannes Gutenberg-Universität Mainz

41st International Symposium on Lattice Field Theory

University of Liverpool, July 28 – August 3, 2024

JOHANNES GUTENBERG
UNIVERSITÄT MAINZ



Introduction

The pion scalar form factor and **scalar radii** with $N_f = 2+1$ quark flavors are given by

$$F_S^{\pi,f}(Q^2) = \langle \pi(p_f) | S^f | \pi(p_i) \rangle, \quad \langle r_S^2 \rangle_\pi^f = \frac{-6}{F_S^{\pi,f}(0)} \cdot \left. \frac{dF_S^{\pi,f}(Q^2)}{dQ^2} \right|_{Q^2=0},$$

where for $f = l, 0, 8$ we have

$$\begin{aligned} S_l &= 2m_l \bar{l}l & \rightarrow & F_S^{\pi,l}(Q^2) & (\text{light}) \\ S_8 &= 2m_l \bar{l}l - 2m_s \bar{s}s & \rightarrow & F_S^{\pi,8}(Q^2) & (\text{octet}) \\ S_0 &= 2m_l \bar{l}l + m_s \bar{s}s & \rightarrow & F_S^{\pi,0}(Q^2) & (\text{singlet}) \end{aligned}$$

They provide insight into the low-energy regime of QCD:

- At NLO in $SU(2)$ χ PT $\langle r_S^2 \rangle_\pi^l$ is parametrized by a single LEC \bar{l}_4 . *Annals Phys.* 158, 142 (1984)
- At NLO in $SU(3)$ χ PT $\langle r_S^2 \rangle_\pi^{0,8,l}$ give access to f_0 , L_4 and L_5 . *Nucl. Phys.* B250 (1985) 517-538
- A few (mostly older) lattice calculations exist for $SU(2)$; very little is known for $SU(3)$.

PRD 80 (2009) 034508

PRD 89 (2014) 9, 094503

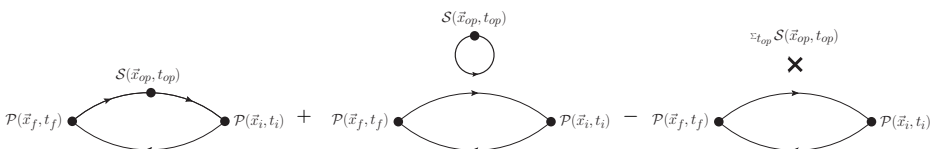
PRD 93 (2016) 5, 054503

PRD 105, 054502 (2022)

- Arguably no calculation with controlled systematics; e.g. radii from linear slope between two momenta.
- $F_S^{\pi,f}(q^2)$ computationally demanding → significant **quark-disconnected contributions**.

Computational setup part I

Contributions from quark-connected and disconnected three-point functions:



- Sequential sink method for three-point functions: $1 \text{ fm} \lesssim t_{\text{sep}} \lesssim 3.5 \text{ fm}$ and $\mathbf{p}_f \in \{(0,0,0), (1,0,0)\}$.
- Truncated solver method → speedup of 2-5. [Phys. Rev. D91 \(2015\) 11, 114511](#)
- Point-to-all forward propagators re-used for two-point functions.
- $\mathcal{O}(500)$ additional two-point functions for 2+1 disconnected diagrams per config.
- On periodic BC boxes:**
 - Sources randomly distributed; 8 sources for quark-connected three-point functions per config.
- On open BC boxes:**
 - Source setup symmetric around $T/2 \Rightarrow 4+4$ sources for three-point functions at each t_{sep} .
 - Additional two-point function sources in bulk, i.e. $t_i \in [t_{\text{ex}}^{\text{oBC}}, T - t_{\text{ex}}^{\text{oBC}}]$, $t_{\text{ex}}^{\text{oBC}} = 1.75 \dots 2.5 \text{ fm}$.

Computational setup part II

Quark-disconnected loops (here: $\mathcal{O}_f(\mathbf{x}, t) = \mathcal{S}_{I,s}(\mathbf{x}, t)$)

$$\mathcal{L}_{\mathcal{O}_f}(\mathbf{p}, t) = \sum_{\mathbf{x}} e^{i\mathbf{p}\cdot\mathbf{x}} \langle \mathcal{O}_f(\mathbf{x}, t) \rangle_F,$$

are computed using **stochastic all-to-all propagators** combining:

- ① the one-end trick / frequency splitting to compute $L_1 - L_2, \dots, L_{n-1} - L_n$, for $m_1 < m_2 < \dots < m_n$

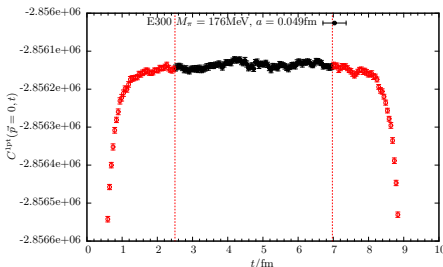
EPJ C58, 261 (2008) *EPJ C79, 586 (2019)*

- ② with the hopping parameter expansion + hierarchical probing for the heaviest quark n .

PRD 89, 094503 (2014) *arXiv:1302.4018 [hep-lat]*

- Loops at gauge noise for any $\mathcal{O}_f(\mathbf{x}, t)$
- Statistics for 2+1 diagrams remains limited by two-point functions measurements.
- For periodic BC: forward + backward averaging for all sources used for two-point functions.
- For open BC: **Stay away from boundary!**

⇒ 2+1 statistics may get severely reduced at larger values of t_{sep} , depending on T and $t_{\text{ex}}^{\text{OBC}}$.



Ensembles

ID ^{BC}	Traj.	a/fm	T/a	L/a	M_π/MeV	$M_\pi L$	N_{conf}	$N_{\text{meas}}^{\text{3pt}}$	$N_{\text{meas}}^{(2+1)\text{pt}}$
C101°	tr[M]	0.086	96	48	225	4.68	2000	16000	800000
C102°	m_s^{phys}		96	48	228	4.75	1500	12000	600000
N101°	tr[M]		128	48	283	5.89	1596	12768	893760
H102°	tr[M]		96	32	358	4.97	2037	16296	1140720
D450 ^P	tr[M]	0.076	128	64	219	5.36	1028	12000	526336
D451 ^P	m_s^{phys}		128	64	218	5.35	1500	8224	768000
N451 ^P	tr[M]		128	48	289	5.32	1011	8088	517632
N452 ^P	tr[M]		128	48	354	6.50	1000	8000	512000
S400°	tr[M]		128	32	356	4.37	1001	8008	448448
E250 ^P	both	0.064	192	96	132	4.07	1000	8000	512000
D200°	tr[M]		128	64	204	4.22	2000	16000	1120000
D201°	m_s^{phys}		128	64	204	4.21	1078	8624	603680
N200°	tr[M]		128	48	287	4.45	1712	13696	958720
N203°	tr[M]		128	48	349	5.40	1543	12344	864080
E300°	tr[M]	0.049	192	96	176	4.22	1139	9112	485973
J303°	tr[M]		192	64	260	4.17	1073	8584	600880

- $N_f = 2 + 1$ flavors of non-perturbatively improved Wilson clover fermions provided by CLS.

JHEP 1502 (2015) 043 Commun.Math.Phys. 97 (1985) PoS LATTICE2008 (2008) 049

- Production almost complete; ensembles only listed if they have reached target statistics.
- 13 Ensembles on $\text{tr}[M] = \text{const}$ trajectory, 3 more on $m_s = m_s^{\text{phys}}$ trajctory.
 → J304 almost done, a few more $m_s = \text{phys}$ ensembles available.

Ensembles

ID ^{BC}	Traj.	a/fm	T/a	L/a	M_π / MeV	$M_\pi L$	N_{conf}	$N_{\text{meas}}^{\text{3pt}}$	$N_{\text{meas}}^{(2+1)\text{pt}}$
C101 ^o	$\text{tr}[M]$	0.086	96	48	225	4.68	2000	16000	800000
C102 ^o	m_s^{phys}		96	48	228	4.75	1500	12000	600000
N101 ^o	$\text{tr}[M]$		128	48	283	5.89	1596	12768	893760
H102 ^o	$\text{tr}[M]$		96	32	358	4.97	2037	16296	1140720
D450 ^P	$\text{tr}[M]$	0.076	128	64	219	5.36	1028	12000	526336
D451 ^P	m_s^{phys}		128	64	218	5.35	1500	8224	768000
N451 ^P	$\text{tr}[M]$		128	48	289	5.32	1011	8088	517632
N452 ^P	$\text{tr}[M]$		128	48	354	6.50	1000	8000	512000
S400 ^o	$\text{tr}[M]$		128	32	356	4.37	1001	8008	448448
E250 ^P	both	0.064	192	96	132	4.07	1000	8000	512000
D200 ^o	$\text{tr}[M]$		128	64	204	4.22	2000	16000	1120000
D201 ^o	m_s^{phys}		128	64	204	4.21	1078	8624	603680
N200 ^o	$\text{tr}[M]$		128	48	287	4.45	1712	13696	958720
N203 ^o	$\text{tr}[M]$		128	48	349	5.40	1543	12344	864080
E300 ^o	$\text{tr}[M]$	0.049	192	96	176	4.22	1139	9112	485973
J303 ^o	$\text{tr}[M]$		192	64	260	4.17	1073	8584	600880

- Ensembles cover four values of the lattice spacing a
- Pion masses range from $\sim 130 \text{ MeV}$ to $\sim 350 \text{ MeV}$
- Many different physical volumes with $L \approx 2.4, \dots, 6.1 \text{ fm}$, $M_\pi L > 4$.
- Two very large and fine boxes at (near) physical quark mass and high momentum resolution.

Ensembles

ID ^{BC}	Traj.	a/fm	T/a	L/a	M_π / MeV	$M_\pi L$	N_{conf}	$N_{\text{meas}}^{\text{3pt}}$	$N_{\text{meas}}^{(2+1)\text{pt}}$
C101 ^o	tr[M]	0.086	96	48	225	4.68	2000	16000	800000
C102 ^o	m_s^{phys}		96	48	228	4.75	1500	12000	600000
N101 ^o	tr[M]		128	48	283	5.89	1596	12768	893760
H102 ^o	tr[M]		96	32	358	4.97	2037	16296	1140720
D450 ^P	tr[M]	0.076	128	64	219	5.36	1028	12000	526336
D451 ^P	m_s^{phys}		128	64	218	5.35	1500	8224	768000
N451 ^P	tr[M]		128	48	289	5.32	1011	8088	517632
N452 ^P	tr[M]		128	48	354	6.50	1000	8000	512000
S400 ^o	tr[M]		128	32	356	4.37	1001	8008	448448
E250 ^P	both	0.064	192	96	132	4.07	1000	8000	512000
D200 ^o	tr[M]		128	64	204	4.22	2000	16000	1120000
D201 ^o	m_s^{phys}		128	64	204	4.21	1078	8624	603680
N200 ^o	tr[M]		128	48	287	4.45	1712	13696	958720
N203 ^o	tr[M]		128	48	349	5.40	1543	12344	864080
E300 ^o	tr[M]	0.049	192	96	176	4.22	1139	9112	485973
J303 ^o	tr[M]		192	64	260	4.17	1073	8584	600880

- Ensembles cover four values of the lattice spacing a
- Pion masses range from $\sim 130 \text{ MeV}$ to $\sim 350 \text{ MeV}$
- Many different physical volumes with $L \approx 2.4, \dots, 6.1 \text{ fm}$, $M_\pi L > 4$.
- Two very large and fine boxes at (near) physical quark mass and high momentum resolution.

Ensembles

ID ^{BC}	Traj.	a/fm	T/a	L/a	M_π / MeV	$M_\pi L$	N_{conf}	$N_{\text{meas}}^{\text{3pt}}$	$N_{\text{meas}}^{(2+1)\text{pt}}$
C101 ^o	tr[M]	0.086	96	48	225	4.68	2000	16000	800000
C102 ^o	m_s^{phys}		96	48	228	4.75	1500	12000	600000
N101 ^o	tr[M]		128	48	283	5.89	1596	12768	893760
H102 ^o	tr[M]		96	32	358	4.97	2037	16296	1140720
D450 ^P	tr[M]	0.076	128	64	219	5.36	1028	12000	526336
D451 ^P	m_s^{phys}		128	64	218	5.35	1500	8224	768000
N451 ^P	tr[M]		128	48	289	5.32	1011	8088	517632
N452 ^P	tr[M]		128	48	354	6.50	1000	8000	512000
S400 ^o	tr[M]		128	32	356	4.37	1001	8008	448448
E250 ^P	both	0.064	192	96	132	4.07	1000	8000	512000
D200 ^o	tr[M]		128	64	204	4.22	2000	16000	1120000
D201 ^o	m_s^{phys}		128	64	204	4.21	1078	8624	603680
N200 ^o	tr[M]		128	48	287	4.45	1712	13696	958720
N203 ^o	tr[M]		128	48	349	5.40	1543	12344	864080
E300 ^o	tr[M]	0.049	192	96	176	4.22	1139	9112	485973
J303 ^o	tr[M]		192	64	260	4.17	1073	8584	600880

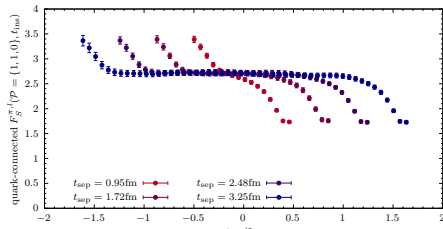
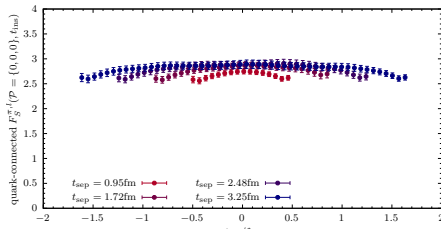
- Ensembles cover four values of the lattice spacing a
- Pion masses range from $\sim 130 \text{ MeV}$ to $\sim 350 \text{ MeV}$
- Many different physical volumes with $L \approx 2.4, \dots, 6.1 \text{ fm}$, $M_\pi L > 4$.
- Two very large and fine boxes at (near) physical quark mass and high momentum resolution.

Ensembles

ID ^{BC}	Traj.	a/fm	T/a	L/a	M_π / MeV	$M_\pi L$	N_{conf}	$N_{\text{meas}}^{\text{3pt}}$	$N_{\text{meas}}^{(2+1)\text{pt}}$
C101 ^o	tr[M]	0.086	96	48	225	4.68	2000	16000	800000
C102 ^o	m_s^{phys}		96	48	228	4.75	1500	12000	600000
N101 ^o	tr[M]		128	48	283	5.89	1596	12768	893760
H102 ^o	tr[M]		96	32	358	4.97	2037	16296	1140720
D450 ^P	tr[M]	0.076	128	64	219	5.36	1028	12000	526336
D451 ^P	m_s^{phys}		128	64	218	5.35	1500	8224	768000
N451 ^P	tr[M]		128	48	289	5.32	1011	8088	517632
N452 ^P	tr[M]		128	48	354	6.50	1000	8000	512000
S400 ^o	tr[M]		128	32	356	4.37	1001	8008	448448
E250 ^P	both	0.064	192	96	132	4.07	1000	8000	512000
D200 ^o	tr[M]		128	64	204	4.22	2000	16000	1120000
D201 ^o	m_s^{phys}		128	64	204	4.21	1078	8624	603680
N200 ^o	tr[M]		128	48	287	4.45	1712	13696	958720
N203 ^o	tr[M]		128	48	349	5.40	1543	12344	864080
E300 ^o	tr[M]	0.049	192	96	176	4.22	1139	9112	485973
J303 ^o	tr[M]		192	64	260	4.17	1073	8584	600880

- Ensembles cover four values of the lattice spacing a
- Pion masses range from $\sim 130 \text{ MeV}$ to $\sim 350 \text{ MeV}$
- Many different physical volumes with $L \approx 2.4, \dots, 6.1 \text{ fm}$, $M_\pi L > 4$.
- Two very large and fine boxes at (near) physical quark mass and high momentum resolution.

Ratio method and effective form factor



Light quark-connected form factors on E250 ($M_\pi = 132$ MeV, $a = 0.064$ fm); momentum labels: $P \equiv (p_f^2, q^2, p_i^2)$

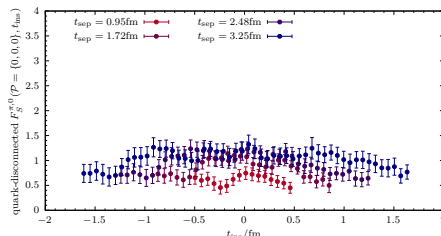
Effective form factors from ratio method:

$$R(p_f^2, q^2, p_i^2, t_f - t_i, t_{op} - t_i) = \frac{C_3(p_f^2, q^2, p_i^2, t_f - t_i, t_{op} - t_i)}{C_2(p_f^2, t_f - t_i)} \sqrt{\frac{C_2(p_i^2, t_f - t_{op}) C_2(p_f^2, t_{op} - t_i) C_2(p_f^2, t_f - t_i)}{C_2(p_f^2, t_f - t_{op}) C_2(p_i^2, t_{op} - t_i) C_2(p_i^2, t_f - t_i)}}.$$

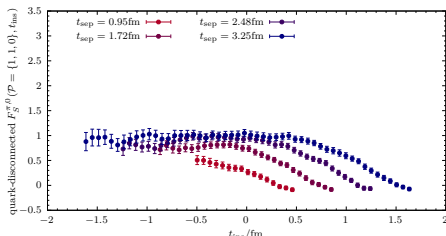
\Rightarrow ground state matrix elements $\langle \pi(p_f^2) | S_f(q^2) | \pi(p_i^2) \rangle \sim F_S^{\pi,f}(Q^2)$ for $t_{op} - t_i \rightarrow \infty$ and $t_f - t_{op} \rightarrow \infty$.

- Quark-connected data very precise at zero- and non-zero Q^2 .

Ratio method and effective form factor



Singlet quark-disconnected form factors on E250 ($M_\pi = 132$ MeV, $a = 0.064$ fm); momentum labels: $\mathcal{P} \equiv (p_f^2, q^2, p_i^2)$



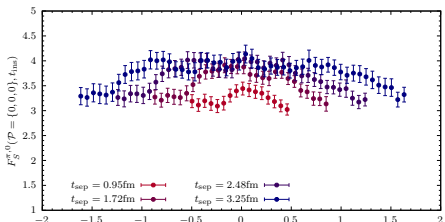
Effective form factors from **ratio method**:

$$R(p_f^2, q^2, p_i^2, t_f - t_i, t_{op} - t_i) = \frac{C_3(p_f^2, q^2, p_i^2, t_f - t_i, t_{op} - t_i)}{C_2(p_f^2, t_f - t_i)} \sqrt{\frac{C_2(p_i^2, t_f - t_{op}) C_2(p_f^2, t_{op} - t_i) C_2(p_f^2, t_f - t_i)}{C_2(p_f^2, t_f - t_{op}) C_2(p_i^2, t_{op} - t_i) C_2(p_i^2, t_f - t_i)}}.$$

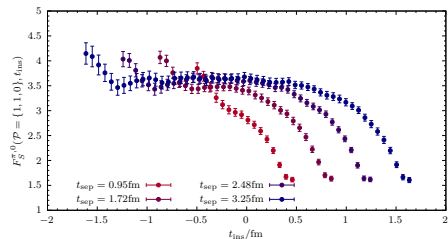
⇒ ground state matrix elements $\langle \pi(p_f^2) | S_f(q^2) | \pi(p_i^2) \rangle \sim F_S^{\pi,f}(Q^2)$ for $t_{op} - t_i \rightarrow \infty$ and $t_f - t_{op} \rightarrow \infty$.

- Quark-connected data very precise at zero- and non-zero Q^2 .
- Quark-disconnected contribution large at small Q^2 → up to $\sim 100\%$ correction on $a = 0.086$ fm.

Ratio method and effective form factor



Full singlet form factors on E250 ($M_\pi = 132$ MeV, $a = 0.064$ fm); momentum labels: $\mathcal{P} \equiv (p_f^2, q^2, p_i^2)$



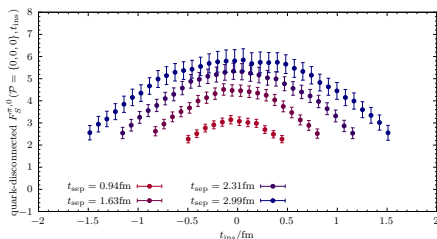
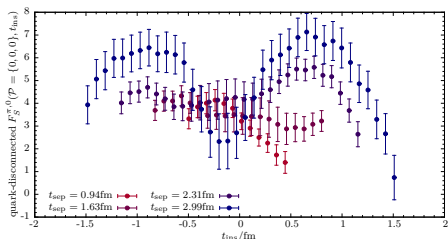
Effective form factors from **ratio method**:

$$R(p_f^2, q^2, p_i^2, t_f - t_i, t_{op} - t_i) = \frac{C_3(p_f^2, q^2, p_i^2, t_f - t_i, t_{op} - t_i)}{C_2(p_f^2, t_f - t_i)} \sqrt{\frac{C_2(p_i^2, t_f - t_{op}) C_2(p_f^2, t_{op} - t_i) C_2(p_f^2, t_f - t_i)}{C_2(p_f^2, t_f - t_{op}) C_2(p_i^2, t_{op} - t_i) C_2(p_i^2, t_f - t_i)}}.$$

⇒ ground state matrix elements $\langle \pi(p_f^2) | S_f(q^2) | \pi(p_i^2) \rangle \sim F_S^{\pi,f}(Q^2)$ for $t_{op} - t_i \rightarrow \infty$ and $t_f - t_{op} \rightarrow \infty$.

- Quark-connected data very precise at zero- and non-zero Q^2 .
- Quark-disconnected contribution large at small $Q^2 \rightarrow$ up to $\sim 100\%$ correction on $a = 0.086$ fm.
- Error of full form factor dominated by disconnected piece.

Technical aside: Vacuum expectation value (VEV) subtraction



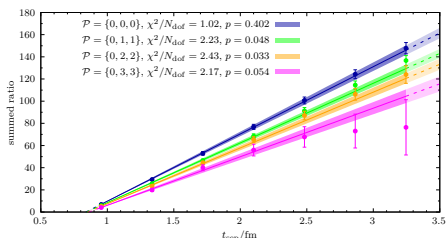
Singlet quark-disconnected contribution at Q^2 on C101 ($M_\pi = 225$ MeV, $a = 0.086$ fm). Left: Standard VEV subtraction. Right: Improved method.

At $Q^2 = 0$ we initially observed large fluctuations in the quark-disconnected signal on **open boundary ensembles**:

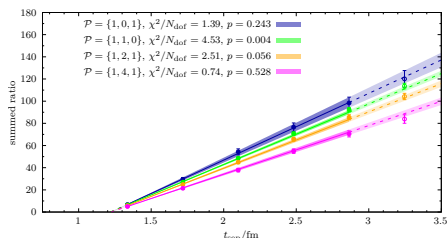
- Correlated fluctuations already visible in the gauge average of the loops (one-point functions).
- Two-point function source-positions t_i often restricted to rather small strip.
- Usual method of (global) VEV-subtraction fails.**
- Instead subtract VEV **per-timeslice**:

$$\left\langle C_{\text{disc}}^{3pt}(t_{\text{sep}}, t_{\text{ins}}) \right\rangle = \frac{1}{N_{t_i}} \sum_{t_i} \left[\left\langle C^{2pt}(t_f - t_i) C^{1pt}(t_{op} - t_i) \right\rangle - \left\langle C^{2pt}(t_f - t_i) \right\rangle \cdot \left\langle C^{1pt}(t_{op} - t_i) \right\rangle \right].$$

Summation method



Summation method for $F_S^{\pi,0}(Q^2)$ on E250 ($M_\pi = 132$ MeV, $a = 0.064$ fm); momentum labels: $\mathcal{P} \equiv (\mathbf{p}_f^2, \mathbf{q}^2, \mathbf{p}_i^2)$



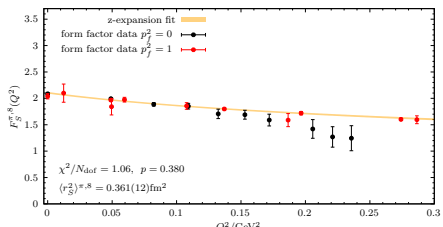
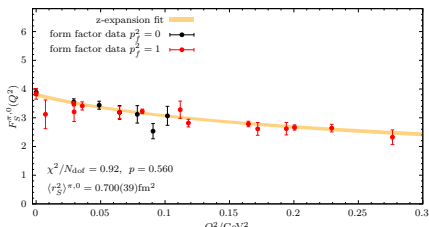
Summation method to extract groundstate matrix elements

$$\sum_{t_{\text{ins}}=t_{\text{ex}}}^{t_{\text{sep}}-t_{\text{ex}}} R(\mathbf{p}_f^2, \mathbf{q}^2, \mathbf{p}_i^2, t_{\text{sep}}, t_{\text{ins}}) = \text{const} + \langle \pi(\mathbf{p}_f^2) | S(Q^2) | \pi(\mathbf{p}_i^2) \rangle (t_{\text{sep}} - t_0) + \mathcal{O}(e^{-\Delta t_{\text{sep}}})$$

- Choose $t_{\text{ex}} \simeq t_{\text{sep}}^{\min}/2$ to improve signal quality for $Q^2 > 0$.
- Use values of $t_{\text{sep}}^{\min} \in [\sim 1.0, \dots, \sim 1.5]$ fm.
- Combined with any $t_{\text{sep}}^{\max} \in [\sim 2.25, \dots, \sim 3.25]$ fm s.t. $t_{\text{sep}}^{\max} - t_{\text{sep}}^{\min} \geq 1$ fm.

→ Carry out remaining analysis for all variations and include them in final model averages

z -expansion fits



Fits for $Q^2 \leq 0.3 \text{ GeV}^2$, $1.25 \lesssim t_{\text{sep}} \lesssim 3.25 \text{ fm}$. Left: $F_S^{\pi,0}(Q^2)$ on E250 ($M_\pi = 132 \text{ MeV}$, $a = 0.064 \text{ fm}$). Right: $F_S^{\pi,8}(Q^2)$ on E300 ($M_\pi = 172 \text{ MeV}$, $a = 0.049 \text{ fm}$)

Use z -expansion to extract radii from **unrenormalized** form factor:

$$F_S^{\pi,f}(Q^2) = \sum_{n=0}^{N_z} a_n z^n, \quad z = \frac{\sqrt{t_{\text{cut}} + Q^2} - \sqrt{t_{\text{cut}} - t_0}}{\sqrt{t_{\text{cut}} + Q^2} + \sqrt{t_{\text{cut}} - t_0}}, \quad a_1 \sim \langle r_S^2 \rangle^f_\pi = -\frac{6}{F_S^{\pi,f}(0)} \cdot \left. \frac{dF_S^{\pi,f}(Q^2)}{dQ^2} \right|_{Q^2=0}$$

We use $N_z = 1$, $t_{\text{cut}} = 4M_\pi^2$ and $t_0 = t_0^{\text{opt}} = t_{\text{cut}}(1 - \sqrt{1 + Q_{\text{max}}^2/t_{\text{cut}}})$.

PRD 92, 013013 (2015)

- Unprecedented Q^2 -resolution at (near) physical quark mass.
- $\mathbf{p}_f = (1, 0, 0)$ data greatly improves signal quality and Q^2 -resolution.
- No renormalization needed for radii.
- Again we apply data cuts, i.e. $Q_{\text{cut}}^2 \in \{0.20, 0.25, 0.30, 0.35, 0.40\} \text{ GeV}^2$.

Physical extrapolation

NLO χ PT fit ansatz with quark mass proxies $m_l \sim M_\pi^2$ and $m_s \sim 2M_K^2 - M_\pi^2$,

$$\begin{aligned}\langle r_S^2 \rangle_\pi^0 &= \frac{1}{(4\pi f_0)^2} \left[768\pi^2 (3L_4^r + L_5^r) - 19 + \frac{m_l}{m_l + 2m_s} - 12 \log(m_l) - 6 \log\left(\frac{m_l + m_s}{2}\right) \right] + c_0 a^2, \\ \langle r_S^2 \rangle_\pi^I &= \frac{1}{(4\pi f_0)^2} \left[768\pi^2 (2L_4^r + L_5^r) - 16 + \frac{m_l}{3(m_l + 2m_s)} - 12 \log(m_l) - 3 \log\left(\frac{m_l + m_s}{2}\right) \right] + c_I a^2, \\ \langle r_S^2 \rangle_\pi^8 &= \frac{1}{(4\pi f_0)^2} \left[768\pi^2 L_5^r - 10 - \frac{m_l}{m_l + 2m_s} - 12 \log(m_l) + 3 \log\left(\frac{m_l + m_s}{2}\right) \right] + c_8 a^2.\end{aligned}$$

- Correlated fits are carried out in units of t_0 with $N_b = 1000$ bootstrap samples.
- Scale setting: $\sqrt{t_0} = 0.14464(87)$ fm. [Eur. Phys. J. C 82 \(2022\) 10, 869 \(FLAG Review 2021\)](#)
- Physical point (isospin limit): $M_\pi^{\text{phys}} = 134.8(3)$ MeV, $M_K^{\text{phys}} = 494.2(3)$ MeV. [Eur. Phys. J. C 77 \(2017\) 2, 112](#)
- Radii are fitted individually to compute $\langle r_S^2 \rangle_{\pi, \text{phys}}^{0,I,8}$.
- LECs f_0 , L_4^r , L_5^r are obtained from fitting the following expressions:

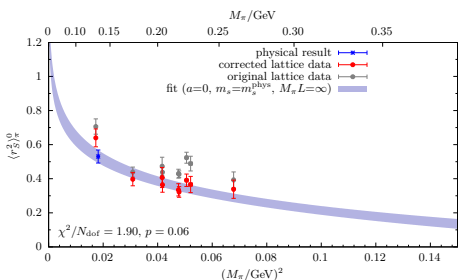
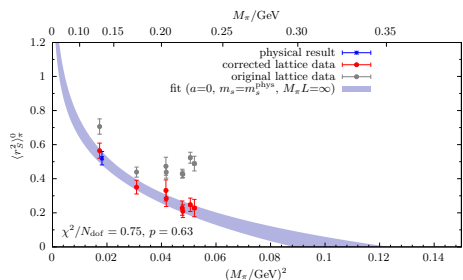
$$f_0 : \langle r_S^2 \rangle_\pi^0, \langle r_S^2 \rangle_\pi^I, \langle r_S^2 \rangle_\pi^8, \langle r_S^2 \rangle_\pi^0 - \langle r_S^2 \rangle_\pi^I, \langle r_S^2 \rangle_\pi^0 - \langle r_S^2 \rangle_\pi^8, \langle r_S^2 \rangle_\pi^I - \langle r_S^2 \rangle_\pi^8,$$

$$L_4^r : \langle r_S^2 \rangle_\pi^0 - \langle r_S^2 \rangle_\pi^I, \langle r_S^2 \rangle_\pi^0 - \langle r_S^2 \rangle_\pi^8, \langle r_S^2 \rangle_\pi^I - \langle r_S^2 \rangle_\pi^8,$$

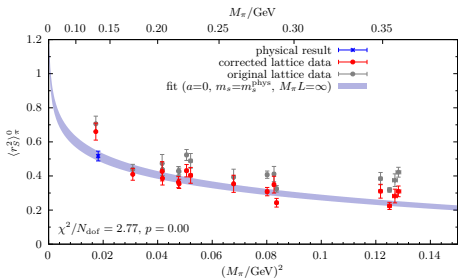
$$L_5^r : \langle r_S^2 \rangle_\pi^8, 3\langle r_S^2 \rangle_\pi^I - 2\langle r_S^2 \rangle_\pi^0$$

- Systematics from (combinations of) data cuts $M_\pi < \{230, 265, 290\}$ MeV, $a < 0.08$ fm and $L > 3.5$ fm.

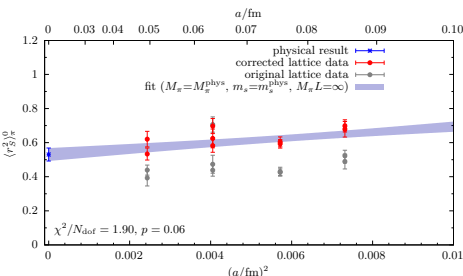
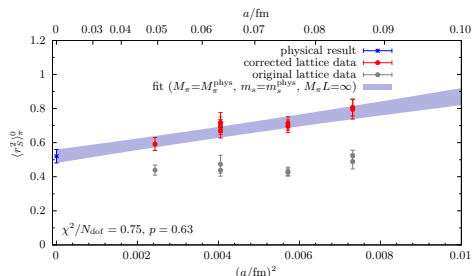
Example: Fit to $\langle r_S^2 \rangle_\pi^0$ data (from $1.5\text{ fm} \lesssim t_{\text{sep}} \lesssim 3.25\text{ fm}$ and $Q^2 \leq 0.3\text{ fm}$)



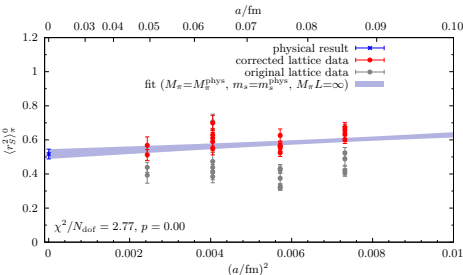
- Data set for $\langle r_S^2 \rangle_\pi^0$ with $1.5\text{ fm} \lesssim t_{\text{sep}} \lesssim 3.25\text{ fm}$ and $Q^2 \leq 0.3\text{ fm}$.
- Steep slope towards chiral limit (chiral log).
- **Pion mass cuts greatly improve fits.**
- E250 falls on fit curve for $M_\pi^{\text{cut}} = 230\text{ MeV}$.
- Data receive significant corrections from fit...



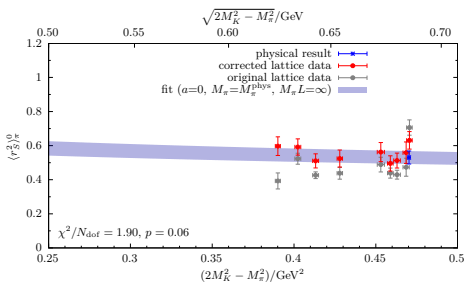
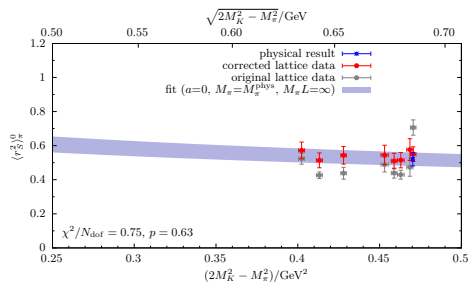
Example: Continuum extrapolation



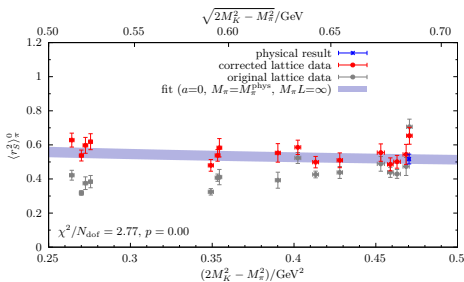
- Corrections dominated by continuum extrapolation.
- (Much) more pronounced for stricter M_π cuts.
→ Higher order corrections?
- Effect from cut $a < 0.08$ fm less severe (not shown).



m_s -dependence



- m_s -depence very mild.
- Cuts in M_π also remove ensembles further away from m_s^{phys} on $\text{tr}[M] = \text{const}$ trajectory
- Physical point in m_s well determined by E250, E300 and ensembles with $m_s \approx \text{phys.}$
- Quite stable under various data cuts.



Model averages

Assign a weight to each model (fit) [Phys. Rev. D 103,114502 \(2021\)](#)

$$w_i \sim \exp \left(-\frac{1}{2} \left[\chi^2 + 2(N_{\text{para}} - N_{\text{prio}}) - 2N_{\text{data}} \right] \right).$$

Central value and total err for an observable y are given by median and 16% and 84% percentiles of the CDF

$$CDF(y, \lambda) = \int_{-\infty}^y d\tilde{y} \sum_i w_i N(\tilde{y}, m_i, \sigma_i \sqrt{\lambda}).$$

Separate statistical (σ_{stat}) and systematic (σ_{sys}) errors from solving

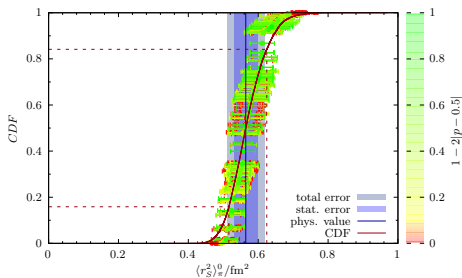
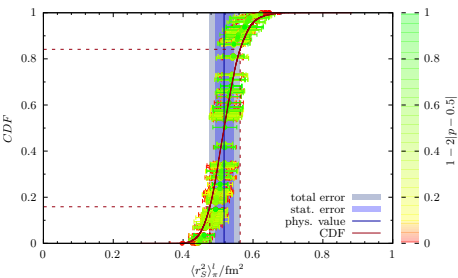
$$\lambda \sigma_{\text{stat}}^2 + \sigma_{\text{sys}}^2 = \left(\frac{y_{\text{hi}} - y_{\text{lo}}}{2} \right)^2 \quad \text{where} \quad CDF(y_{\text{hi}}, \lambda) = 0.84, \quad \text{and} \quad CDF(y_{\text{lo}}, \lambda) = 0.16,$$

where $\lambda = 2.0$ rescales the statistical errors [Nature 593 \(2021\) 7857, 51-55](#)

Final set of models: $\underbrace{\{(t_{\text{sep}}^{\min}, t_{\text{sep}}^{\max})\text{-pairs}\}}_{\text{summation method}} \otimes \underbrace{\{Q^2\text{-cuts}\}}_{\text{z-expansion}} \otimes \underbrace{\{M_{\pi^-}, a\text{- and } L\text{-cuts}\}}_{\text{physical extrapolation}}$

observable	$\langle r_S^2 \rangle_{\pi, \text{phys}}^{0, l, 8}$	f_0	L'_4	L'_5
#models	910	5460	2730	1820

Results for radii



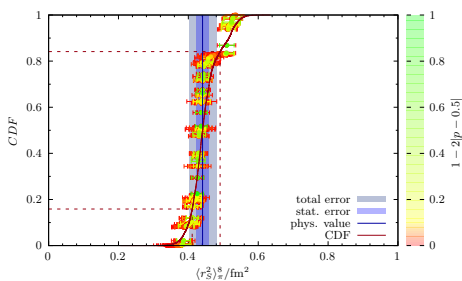
• Results for radii (preliminary):

$$\langle r_S^2 \rangle_\pi^0 = 0.564(34)_{\text{stat}}(42)_{\text{sys}} \text{ fm}^2,$$

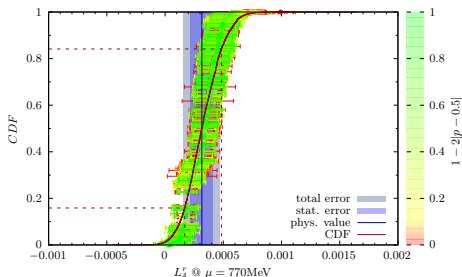
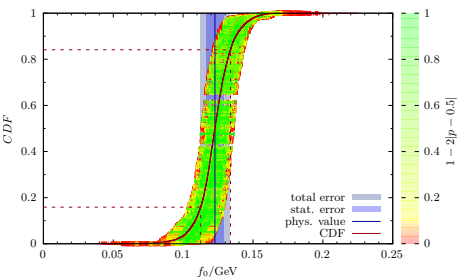
$$\langle r_S^2 \rangle_\pi^I = 0.517(28)_{\text{stat}}(33)_{\text{sys}} \text{ fm}^2,$$

$$\langle r_S^2 \rangle_\pi^8 = 0.441(18)_{\text{stat}}(36)_{\text{sys}} \text{ fm}^2.$$

- Error for $\langle r_S^2 \rangle_\pi^8$ dominated by systematics.
- Expected hierarchy: $\langle r_S^2 \rangle_\pi^8 < \langle r_S^2 \rangle_\pi^I < \langle r_S^2 \rangle_\pi^0$.
- Compatible with only other lattice calculation by HPQCD. *Phys. Rev. D93, 054503 (2016)*



Results for LECs



- **Results for LECs @ $\mu = 770$ MeV (preliminary):**

$$f_0 = 122.7(6.5)_{\text{stat}}(8.5)_{\text{sys}} \text{ MeV}$$

$$L_4^r(\mu) = +0.32(10)_{\text{stat}}(12)_{\text{sys}} \times 10^{-3}$$

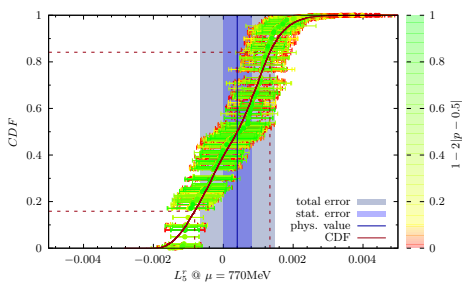
$$L_5^r(\mu) = +0.40(41)_{\text{stat}}(1.00)_{\text{sys}} \times 10^{-3}$$

- FLAG 2021 estimates ($N_f = 2+1$):

$$f_0 = 114.0(8.5) \text{ MeV}$$

$$L_4^r(\mu) = -0.02(56) \times 10^{-3}$$

$$L_5^r(\mu) = +0.95(41) \times 10^{-3}$$



Summary and Outlook

- **Study of the pion scalar radii on 16 CLS $N_f = 2+1$ ensembles:**
 - Results for radii at the physical point and results for $SU(3)$ χ PT LECs.
 - **First calculation with fully controlled systematics and corresponding error budget, i.e. excited states, momentum dependence and physical extrapolation.**
 - Most precise existing determination of L_4^r .
- **Future plans:**
 - Finish production and carry out final analysis.
 - Dedicated determination of \bar{l}_4 from $SU(2)$ χ PT fit.
→ possibly add a few more ensembles on m_s^{phys} -trajectory.
 - Analyze further form factors, e.g. $F_V^{\pi,K}(Q^2)$.
→ data for all 16 local and one-link displaced operator insertions